Inorganic Chemistry

ARTICLE

pubs.acs.org/IC

Density Functional Analysis of the Magnetic Structure of Li_3RuO_4: Importance of the Ru−O···O−Ru Spin-Exchange Interactions and Substitutional Ru Defects at the Li Sites

Won-Joon Son,[†] Pascal Manuel,[‡] Devashibhai Adroja,[‡] and Myung-Hwan Whangbo[†,*]

[†]Department of Chemistry, North Carolina State University, Raleigh, North Carolina 27695-8204, United States

[‡]ISIS Facility, Rutherford Appleton Laboratory, Chilton, Didcot, Oxon, OX11 0QX, United Kingdom

ABSTRACT: We evaluated the spin-exchange interactions of Li_3RuO_4 by performing energy-mapping analysis based on density functional calculations and examined the nature of its magnetic transition at $T_1 = 66$ K and the divergence of the field-cooled and zero-field-cooled susceptibilities below $T_2 = 32$ K. Our study shows that T_1 is associated with a three-dimensional antiferromagnetic ordering, in which the two-dimensional antiferromagnetic lattices parallel to the *ab* plane are antiferromagnetically coupled along the *c* direction. We examined how the substitutional defects, Ru atoms residing in the Li sites, affect the antiferromagnetic coupling along the *c* direction to explain why the expected *c*-axis doubling is not detected from powder neutron diffraction measurements. The susceptibility divergence below T_2 is attributed to a slight spin canting out of the *ab* plane.

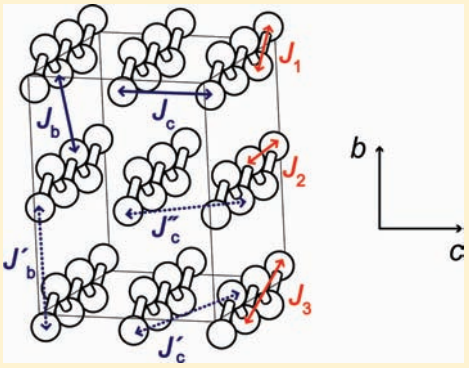

1. INTRODUCTION

The low-lying excited states of a magnetic solid are generally described in terms of a spin Hamiltonian defined with a set of spin-exchange parameters J.[1] The latter are numerical fitting parameters needed to reproduce its magnetic data such as magnetic susceptibility, magnetization, specific heat, and spin wave dispersion relation. These "experimental" J values depend on the set of spin-exchange paths (i.e., the spin−lattice) used to define the spin Hamiltonian. If one selects the spin−lattice by merely inspecting the geometrical pattern of the magnetic ion arrangement or by seeking the novelty of the physics the chosen model might generate, interpretations irrelevant for a given magnetic solid often result, as found for $(VO)_2P_2O_7$,[2,3] $Na_3Cu_2SbO_6$ and $Na_2Cu_2TeO_6$,[4−8] $Bi_4Cu_3V_2O_{14}$,[9−12] azurite $Cu_3(CO_3)_2(OH)_2$,[13−15] and $Cu_3(P_2O_6OH)_2$.[16−18] For magnetic oxides of transition-metal ions M^{n+}, spin-exchange interactions are determined primarily by the magnetic orbitals of its magnetic ions, which are highly anisotropic in shape so that the interaction between the magnetic orbitals of two neighboring magnetic ions is not necessarily stronger when the distance between the ions is shorter.[1] Therefore, it is important to determine the spin−lattice of a magnetic solid on the basis of appropriate electronic structure calculations.

The 4d oxide Li_3RuO_4 consists of isolated zigzag RuO_4 chains that are made up of edge-sharing RuO_6 octahedra with Ru^{5+} (d^3) ions.[19] These chains, running along the *a*-axis direction, are interconnected by Li^+ ions located at the octahedral sites between the zigzag RuO_4 chains. The magnetic properties of Li_3RuO_4 were examined by Alexander et al.[19] and by Soma and Sato.[20] The magnetic susceptibility data of Alexander et al. showed a local maximum at $T_1 \approx 50$ K and divergence of the field-cooled (FC) and zero-field-cooled (ZFC) susceptibilities below $T_2 \approx 20$ K. The susceptibility peak at T_1 is not a broad maximum expected for the short-range order in low-dimensional magnetic systems but has a sharp bend below T_1. Nevertheless, their neutron diffraction study at 5 K did not detect any additional magnetic Bragg peaks, thereby suggesting that the anomaly at T_1 is caused by a short-range order. Re-examination of the magnetic properties of Li_3RuO_4 by Soma and Sato[20] found that $T_1 = 66$ K, $T_2 = 32$ K, and the magnetic susceptibility above 100 K follows a Curie−Weiss behavior with Curie−Weiss temperature $\theta = -231$ K. In their specific heat measurements for Li_3RuO_4,[20] Soma and Sato detected a clear anomaly at T_1 and hence concluded that T_1 is due to a three-dimensional (3D) antiferromagnetic (AFM), namely, T_1 is the Néel temperature. Thus, they suggested[20] that the Ru^{5+} ions of the one-dimensional (1D) zigzag RuO_4 chains have substantial interchain spin-exchange interactions, and some spin frustration[21,22] exists in Li_3RuO_4 because T_1 is small compared with $|\theta|$ (i.e., $|\theta|/T_1 = 3.5$). The origin of the magnetic behavior below T_2 is not clear.[20] Thus, a Heisenberg 1D AFM chain model does not seem appropriate for Li_3RuO_4 although, geometrically, it consists of zigzag chains of Ru^{5+} ions.

In the spin-exchange interactions of many transition metal oxides, the M−O···O−M spin exchanges are often stronger than the M−O−M spin exchanges.[1] Furthermore, a recent study of Na_3RuO_4,[23] which consists of Ru_4O_{16} clusters made up of edge-sharing RuO_6 octahedra with Ru^{5+} (d^3) ions, showed that

Received: May 14, 2011
Published: August 11, 2011

the intercluster spin exchanges through the Ru−O···O−Ru paths are much stronger than the intracluster spin exchanges through the Ru−O−Ru paths. Thus, it is expected that the interchain Ru−O···O−Ru spin-exchange interactions play an important role in determining the magnetic structure of Li_3RuO_4. In the present work we explore what kind of magnetic ordering is responsible for the T_1 transition of Li_3RuO_4 and how such a magnetic ordering can be compatible with the neutron diffraction study of Alexander et al.[19] as well as that of the recent neutron diffraction/scattering study of Manuel et al.[24] Thus, we evaluate the spin-exchange interactions of Li_3RuO_4 by performing energy-mapping analysis based on density functional calculations and discuss the aforementioned questions in terms of the spin-exchange parameters extracted in the present study.

2. EVALUATION OF SPIN-EXCHANGE PARAMETERS

For the spin-exchange paths of Li_3RuO_4, we consider three intrachain (J_1, J_2, and J_3) and five interchain (J_b and J'_b along the b direction as well as J_c, J'_c, and J''_c along the c direction) paths defined in Figure 1. The geometrical parameters associated with these spin-exchange paths, taken from the room-temperature crystal structure of Li_3RuO_4,[19] are summarized in Table 1. For our density functional calculations, we employed the crystal structure of Li_3RuO_4 determined at 70 K.[24] As compared in Table 1, the room-temperature and 70 K crystal structures give quite similar structural parameters for the eight spin-exchange paths. The spin-exchange parameters for these paths were evaluated by performing energy-mapping analysis based on density functional calculations.[1] We first determine the relative energies of the nine ordered spin states of Li_3RuO_4, namely, the ferromagnetic (FM) state plus the eight states AF1−AF8 defined in terms of a (3a, 2b, 2c) supercell (Figure 2) containing 24 formula units (FUs). In our density functional calculations, we employed the projector-augmented wave (PAW) method encoded in the Vienna ab initio simulation package (VASP)[25−27] and the generalized-gradient approximation (GGA) of Perdew, Burke, and Ernzerhof[28] for the exchange-correlation functional with the plane-wave cutoff energy of 485 eV, a set of $3 \times 4 \times 4$ k points for the irreducible Brillouin zone, and a self-consistent-field energy convergence threshold of 10^{-6} eV. The 4d and 5d orbitals are more diffuse than the 3d orbitals, so that electron localization is less likely for 4d and 5d than for 3d metal elements. Nevertheless, the oxides of Ru and Os in high oxidation state are magnetic insulators because their 4d and 5d orbitals are contracted.[29,30] To probe the possible effect of electron correlation associated with the 4d states of the Ru^{5+} ions in Li_3RuO_4, the GGA plus on-site repulsion U (GGA+U)[31] calculations were also carried out with U = 1 and 3 eV. Figure 3 shows plots of the density of states obtained for the FM state of Li_3RuO_4 from GGA+U calculations. As expected, the band gap increases on increasing the value of U.

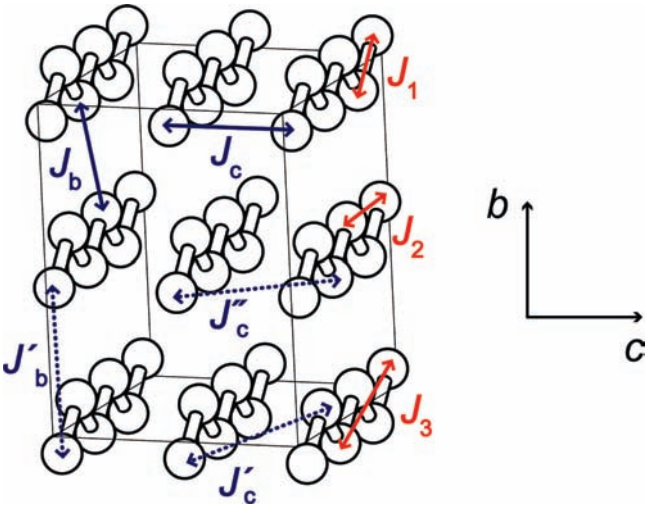

Figure 1. Definition of the eight spin-exchange paths considered for Li_3RuO_4 using a $3 \times 2 \times 2$ supercell. For simplicity, only the Ru^{5+} ions are shown.

The relative energies of the eight spin-ordered states AF1−AF8 with respect to the FM state are given in Table 2. The total spin-exchange energies of the nine ordered spin states can be written in terms of the spin Hamiltonian

$$\hat{H} = -\sum_{i<j} J_{ij} \hat{S}_i \cdot \hat{S}_j \qquad (1)$$

in which J_{ij} (=J_1, J_2, J_3, J_b, J'_b, J_c, J'_c, and J''_c) is the exchange parameter for the interaction between spin sites i and j in Li_3RuO_4. By applying the energy expressions obtained for spin dimers with N unpaired spins per spin site (in the present case, N = 3),[32,33] the total spin-exchange energies (per 24 FUs) of the nine ordered spin states are written as summarized in Table 2. Then, by mapping the relative energies of the nine spin-ordered states determined from the GGA+U calculations onto the corresponding energies expected from the total spin-exchange energies, we obtain the values of the eight spin-exchange parameters summarized in Table 3.

3. SPIN−LATTICE OF LI_3RUO_4

It is known that the values of spin-exchange parameters are overestimated by GGA+U calculations by a factor of up to four and decrease with increasing U value.[7,12,34] Given the three sets of

Table 1. Geometrical Parameters Associated with the Eight Spin-Exchange Paths of Li_3RuO_4 Taken from the Room-Temperature Structure of Alexander et al. (ref 19) and the 70 K Structure of Manuel et al. (ref 24)

	Ru···Ru	geometry
J_1	2.990 [2.989]	Ru−O = 1.975 [1.970] Å, 1.998 [2.004] Å, ∠Ru−O−Ru = 97.6° [97.6°]
J_2	5.106 [5.099]	O···O = 2.799 [2.828] Å, ∠Ru−O···O = 97.0 [96.6]
J_3	7.815 [7.806]	O···O = 5.106 [5.099] Å, ∠Ru−O···O = 116.7° [117.0°], 146.8° [146.3°]
J_b	4.999 [4.988]	O···O = 3.045 [3.022] Å, ∠Ru−O···O = 92.1° [92.5°]
J'_b	5.854 [5.847]	O···O = 3.104 [3.101] Å, ∠Ru−O···O = 135.2° [134.2°], 133.4° [134.3°]
J_c	5.106 [5.099]	O···O = 3.076 [3.040] Å, ∠Ru−O···O = 92.6°
J'_c	5.107 [5.102]	O···O = 3.076 Å, ∠Ru−O···O = 92.6° [93.1°], 133.7° [134.1°]
J''_c	5.854 [5.847]	O···O = 3.076 [3.040] Å, 3.067 [3.089] Å, ∠Ru−O···O = 133.7° [134.1°], 136.2° [135.9°]

dx.doi.org/10.1021/ic201023j |Inorg. Chem. 2011, 50, 9400–9405

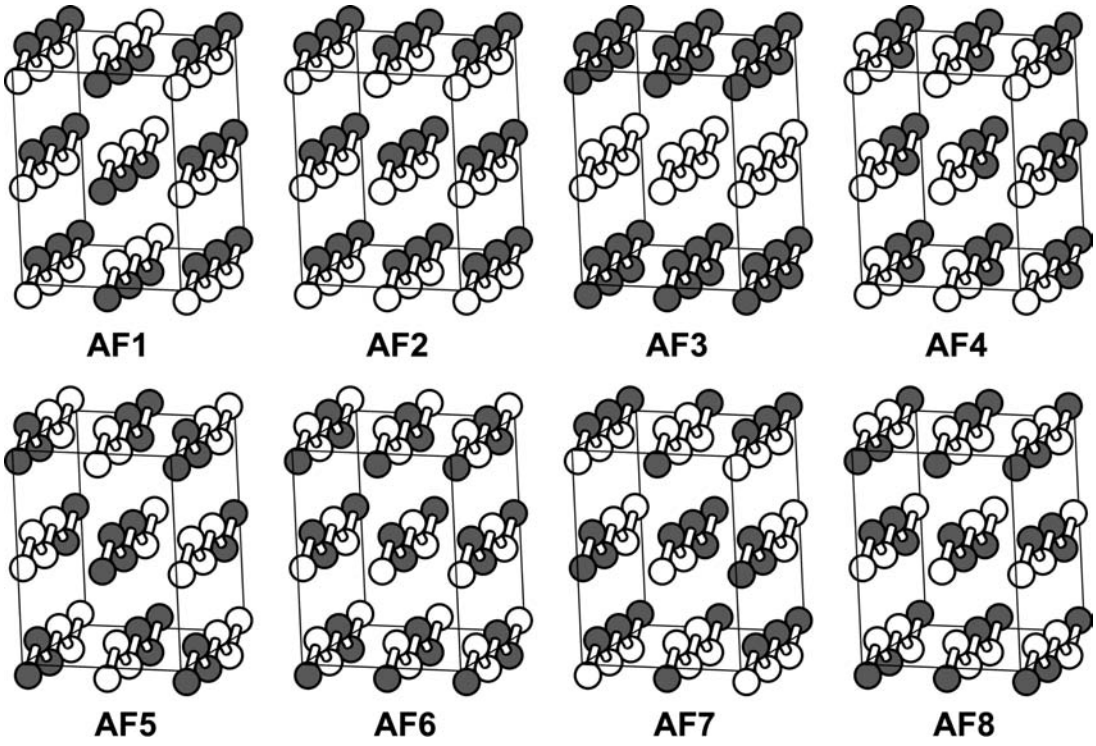

Figure 2. Spin arrangements of the ordered spin states AF1−AF8 of Li_3RuO_4, where the filled and empty circles represent the down-spin and up-spin Ru^{5+} sites, respectively. The FM state in which all Ru^{5+} sites have an identical spin is not shown.

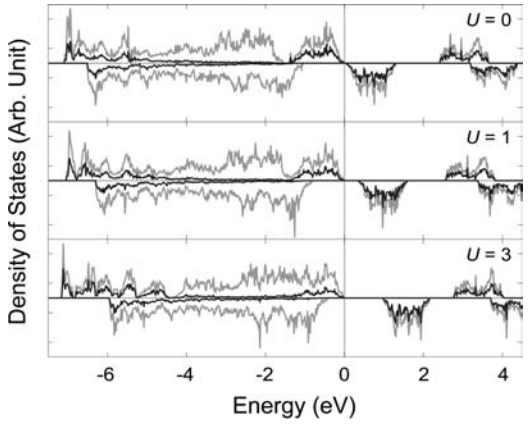

Figure 3. Density of states calculated for the FM state of Li_3RuO_4 by GGA+U calculations with U = 0, 1, and 3 eV. The total density of states is shown by gray curves and the projected density of states for the Ru 4d orbitals by black curves. The Fermi level is indicated by the vertical line.

spin-exchange parameters obtained from the GGA+U calculations with U = 0, 1, and 3 eV, one needs to find which set is most appropriate for Li_3RuO_4. For this purpose, we calculate the Curie−Weiss temperature θ using the mean field approximation,[35] namely

$$\theta = \frac{S(S+1)}{3k_B}\sum_i z_i J_i \qquad (2)$$

where the summation runs over all nearest neighbors of a given spin site, z_i is the number of nearest neighbors connected by the spin-exchange parameter J_i, and S is the spin quantum number of each spin site (i.e., S = 3/2 for Ru^{5+}). Thus, for Li_3RuO_4, θ is written as

$$\theta \approx 5(J_1 + J_2 + J_3 + J_b + J_b' + J_c + J_c' + J_c'')/2k_B \qquad (3)$$

and hence we obtain θ = −641, −439, and −218 K by using the spin-exchange parameters obtained from the GGA+U calculations with U = 0, 1, and 3 eV, respectively. Given that θ = −231 K experimentally, the spin exchanges obtained from the use of U = 3 eV are most appropriate for Li_3RuO_4 and hence will be used in our subsequent discussion.

Among the eight spin exchanges, the three strongest ones are J_1, J_2, and J_b with their strengths decreasing in the order $J_1 > J_b > J_2$. As depicted in Figure 4, the J_1 and J_b exchanges form a 2D AFM quadrangular lattice parallel to the *ab* plane while the J_2 exchange leads to spin frustration in each quadrangle. Such spin-frustrated 2D AFM quadrangular lattices are antiferromagnetically coupled along the *c* direction by the weak AFM exchange J_c to form a 3D AFM lattice. This is in support of the suggestion that T_1 is the 3D AFM ordering temperature of Li_3RuO_4.

4. DISCUSSION

According to the above explanation for the T_1 transition, the *c*-axis length should be doubled in the 3D ordered structure below T_1. However, in the powder neutron diffraction measurements of Alexander et al.,[19] the *c*-axis doubling was not detected. This is also the case in the recent neutron diffraction study of Manuel et al.,[24] although they observed magnetic Bragg peaks associated with a 3D AFM magnetic ordering. To account for why the *c*-axis doubling predicted from our calculations is not found in the neutron diffraction studies, we examine how

dx.doi.org/10.1021/ic201023j |*Inorg. Chem.* 2011, 50, 9400–9405

Table 2. Total Spin-Exchange Energies (in terms of the eight spin-exchange parameters) and Relative Energies (determined from the GGA+U calculations) for the Nine Ordered Spin States of Li_3RuO_4[a]

	total spin-exchange energy	relative energy (in eV)
FM	$-(24J_1 + 24J_2 + 24J_3 + 24J_b + 24J'_b + 24J_c + 24J'_c + 24J''_c)(N^2/4)$	(0.00, 0.00, 0.00)
AF1	$-(-24J_1 + 24J_2 - 24J_3 - 24J_b + 24J'_b - 24J_c + 24J'_c - 24J''_c)(N^2/4)$	(−1.98, −1.32, −0.61)
AF2	$-(-24J_1 + 24J_2 - 24J_3 - 24J_b + 24J'_b + 24J_c - 24J'_c + 24J''_c)(N^2/4)$	(−1.93, −1.28, −0.58)
AF3	$-(24J_1 + 24J_2 + 24J_3 - 24J_b - 24J'_b + 24J_c + 24J'_c + 24J''_c)(N^2/4)$	(−0.60, −0.44, −0.27)
AF4	$-(8J_1 - 8J_2 - 24J_3 + 8J_b + 24J'_b + 24J_c + 8J'_c - 8J''_c)(N^2/4)$	(−0.89, −0.62, −0.32)
AF5	$-(8J_1 - 8J_2 - 16J_3 - 8J_b - 16J'_b - 24J_c - 8J'_c + 8J''_c)$	(−1.19, −0.84, −0.45)
AF6	$-(-8J_1 - 8J_2 + 8J_3 + 8J_b - 24J'_b + 24J_c - 8J'_c - 8J''_c)(N^2/4)$	(−1.43, −0.96, −0.46)
AF7	$-(-4J_1 + 4J_2 - 16J_3 + 4J_b - 8J'_b - 8J_c)(N^2/4)$	(−1.32, −0.89, −0.43)
AF8	$-(-8J_1 - 8J_2 + 8J_3 + 8J_b - 24J'_b + 8J_c - 8J''_c)(N^2/4)$	(−1.45, −0.98, −0.47)

[a] The three values (from left to right) of the relative energy for each state are obtained from the GGA+U calculations with $U = 0$, 1, and 3 eV, respectively. All expressions and relative energies are per $3 \times 2 \times 2$ supercell (i.e., per 24 FUs).

Table 3. Values of the Eight Spin-Exchange Parameters (in meV) of Li_3RuO_4 Obtained from the Mapping Analysis Based on the GGA+U Calculations

	$U = 0$ eV	$U = 1$ eV	$U = 3$ eV
J_1	−13.04	−8.16	−3.13
J_2	−2.66	−2.12	−1.37
J_3	−1.05	−0.62	−0.30
J_b	−4.12	−3.16	−1.96
J'_b	−1.42	−0.92	−0.53
J_c	−0.35	−0.34	−0.23
J'_c	+0.31	+0.12	+0.03
J''_c	+0.23	+0.07	−0.03

substitutional defects of Li_3RuO_4, namely, Ru atoms residing in the Li sites,[20] might affect the magnetic ordering along the c direction. In the neutron diffraction studies of Alexander et al.[19] and Manuel et al.,[24] the possible occurrence of substitutional defects in their Li_3RuO_4 samples was not investigated. As shown in Table 3, the Ru−O···Li···O−Ru spin exchange J_c is weakly antiferromagnetic. However, if the Li site of this exchange path is occupied by a Ru atom, the resulting exchange path Ru−O···Ru···O−Ru leads to a FM coupling between the two chains along the c direction provided that the Ru−O···Ru spin exchange is AFM. The latter is most likely the case given the fact that the Ru−O−Ru superexchange J_1 is AFM. Then, the sense of the interchain AFM coupling along the c direction is randomly reversed by defect Ru atoms residing at the Li sites. In such a case, powder neutron diffraction measurements cannot detect the c-axis doubling.

In principle, either spin frustration or spin canting can be a cause for the divergence of the FC and ZFC susceptibilities below T_2. In the present case, spin frustration cannot cause the divergence below T_2, because Li_3RuO_4 undergoes a 3D AFM ordering below T_1. The recent neutron diffraction study[24] of Li_3RuO_4 shows no canting of the ordered moments, so spin canting does not appear to be responsible for the susceptibility divergence below T_2. However, we note that the expected c-axis doubling was not detected in this neutron diffraction study, which is due probably due to defect Ru atoms residing at the Li sites as suggested above. If the spin canting is out of the ab plane, such defects can also randomly reverse the direction of the spin canting so that powder neutron diffraction measurements cannot detect the spin canting.

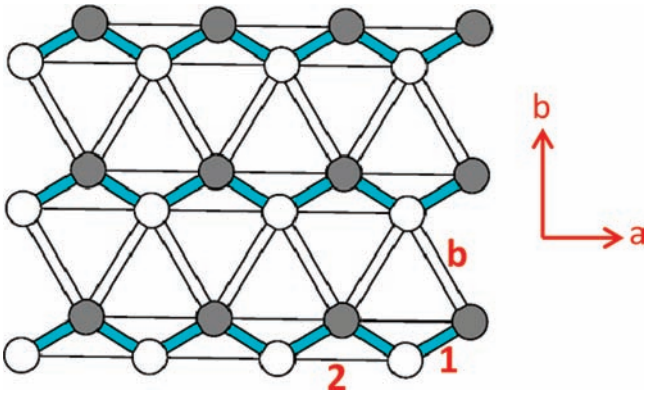

Figure 4. Two-dinensional quadrangular AFM lattice of Li_3RuO_4 parallel to the ab plane, which is defined by the intrachain exchange J_1 and the interchain exchange J_b. The labels 1, 2, and b represent the spin exchanges J_1, J_2, and J_b, respectively. The intrachain spin exchange J_2 leads to spin frustration in the (J_1, J_1, J_2) and (J_b, J_b, J_2) triangles. Such 2D lattices are expected to be antiferromagnetically coupled by J_c along the c direction in the 3D AFM structure of Li_3RuO_4 below $T_1 = 66$ K.

It is of interest to examine what kinds of spin-exchange parameters might result when the 3D spin−lattice of Li_3RuO_4 is approximated by a 2D lattice or a 1D chain model. Thus, we extract the J_1, J_2, J_3, and J_b values using a 2D lattice model and J_1, J_2, and J_3 values for a 1D chain model. In extracting these spin-exchange parameters, we employ all the nine spin-ordered states used for extracting the eight spin exchanges for the 3D spin−lattice. Since we have more states than needed for one-to-one mapping, we carry out least-squares fitting analyses. (In extracting the three spin exchanges of the 1D chain model, the AF3 state was excluded because it becomes identical to the FM state in this model.) The spin-exchange parameters deduced for the 2D lattice and 1D chain models by least-squares fitting analyses are summarized in Table 4a and 4b, respectively. Table 4c compares the spin-exchange parameters obtained for the 3D, 2D, and 1D models from the GGA+U calculations with $U = 3$ eV. As expected, the 2D model provides the spin exchanges close to those deduced for the 3D model, except that J_3 becomes weakly FM. The 1D model provides a striking change in the intrachain exchange J_3, which becomes strongly AFM, that is, J_3 becomes almost comparable in magnitude to J_2. It appears that the deficiency of the 1D model is compensated by making J_3 strongly AFM. This suggestion

dx.doi.org/10.1021/ic201023j |Inorg. Chem. 2011, 50, 9400–9405

Table 4. Spin-Exchange Parameters of Li_3RuO_4 (in meV) Obtained for the 2D and 1D Spin−Lattice Models by Least-Squares Fitting analyses (where R^2 is a parameter for the goodness of fitting)

(a) for the 2D spin−lattice

U (eV)	J_1	J_2	J_3	J_b	R^2
0	−13.03	−4.50	+0.37	−5.56	0.99
1	−8.22	−3.40	+0.25	−4.12	0.99
3	−3.22	−2.16	+0.17	−2.51	0.97

(b) for 1D spin−lattice

U (eV)	J_1	J_2	J_3	R^2
0	−15.85	−3.25	−2.18	0.94
1	−10.31	−2.48	−1.64	0.91
3	−4.49	−1.59	−0.98	0.78

(c) spin-exchange parameters of the 3D, 2D, and 1D spin−lattice models from the GGA+U calculations with U = 3 eV

	3D	2D	1D
J_1	−3.13	−3.22	−4.49
J_2	−1.37	−2.16	−1.59
J_3	−0.30	+0.17	−0.98
J_b	−1.96	−2.51	0.00

is in agreement with the results of the recent neutron scattering study of Li_3RuO_4 by Manuel et al.[24] Their analysis of the spin wave dispersion relations by using a 1D Heisenberg chain model shows the spin-exchange parameters J_1, J_2, and J_3 to be −3.3(1), −1.4(1), and −1.2(1) meV, respectively. These values are very similar to those obtained in our calculations using a 1D chain model (−4.49, −1.59, and −0.98 meV, respectively).

5. CONCLUDING REMARKS

The spin-exchange parameters of Li_3RuO_4 extracted from our density functional calculations show that T_1 is associated with the 3D AFM ordering, in which the 2D AFM lattices parallel to the *ab* plane, formed by the intrachain exchange J_1 and the interchain exchange J_b, are coupled antiferromagnetically by J_c along the *c* direction. It is most likely that the substitutional defects, Ru atoms present at the Li sites, are responsible for the absence of the predicted *c*-axis doubling in the powder neutron diffraction studies, because they can randomly reverse the sense of the interchain AFM coupling along the *c* direction. The divergence between the FC and the ZFC susceptibilities below T_2 can be explained if spin canting out of the *ab* plane takes place below. The absence of spin canting in the powder neutron diffraction study[24] would be a consequence of the substitutional Ru defects because they will randomly reverse the directions of the spin canting. In resolving the discrepancy between the experimental and the theoretical magnetic structures of Li_3RuO_4, it is desirable to have samples of Li_3RuO_4 free of substitutional defects and verify the role of the substitutional defects suggested in the present work.

AUTHOR INFORMATION

Corresponding Author

*E-mail: mike_whangbo@ncsu.edu.

ACKNOWLEDGMENT

Work at NCSU by the Office of Basic Energy Sciences, Division of Materials Sciences, U.S. Department of Energy, under Grant DE-FG02-86ER45259, and also by the computing resources of the NERSC center and the HPC center of NCSU is acknowledged.

REFERENCES

(1) Whangbo, M.-H.; Koo, H.-J.; Dai, D. *J. Solid State Chem.* **2003**, *176*, 417.
(2) Garret, A. W.; Nagler, S. E.; Tennant, D. A.; Sales, B. C.; Barnes, T. *Phys. Rev. Lett.* **1997**, *79*, 745.
(3) Koo, H.-J.; Whangbo, M.-H.; VerNooy, P. D.; Torardi, C. C.; Marshall, W. J. *Inorg. Chem.* **2002**, *41*, 4664.
(4) Xu, J.; Assoud, A.; Soheilnia, N.; Derakhshan, S.; Cuthbert, H. L.; Greedan, J. E.; Whangbo, M.- H.; Kleinke, H. *Inorg. Chem.* **2005**, *44*, 5042.
(5) Miura, Y.; Hirai, R.; Kobayashi, Y.; Sato, M. *J. Phys. Soc. Jpn.* **2006**, *75*, 84707.
(6) Derakhshan, S.; Cuthbert, H. L.; Greedan, J. E.; Rahman, B.; Saha-Dasgupta, T. *Phys. Rev. B* **2007**, *76*, 104403.
(7) Koo, H.-J.; Whangbo, M.-H. *Inorg. Chem.* **2008**, *47*, 128.
(8) Miura, Y.; Yasui, Y.; Moyoshi, T.; Sato, M.; Kakurai, K. *J. Phys. Soc. Jpn.* **2008**, *77*, 104789.
(9) Sakurai, H.; Yoshimura, K.; Kosuge, K.; Tsujii, N.; Abe, H.; Kitazawa, H.; Kido, G.; Michor, H.; Hilscher, G. *J. Phys. Soc. Jpn.* **2002**, *71*, 1161.
(10) Okubo, S.; Hirano, T.; Inagaki, Y.; Ohta, H.; Sakurai, H.; Yoshimura, H.; Kosuge, K. *Physica B* **2004**, *346*, 65.
(11) Okamoto, K.; Tonegawa, T.; Kaburagi, M. *J. Phys.: Condens. Matter* **2003**, *15*, 5979.
(12) Koo, H.-J.; Whangbo, M.-H. *Inorg. Chem.* **2008**, *47*, 4779.
(13) Kikuchi, H.; Fujii, Y.; Chiba, M.; Mitsudo, S.; Idehara, T. *Physica B* **2003**, *329*−*333*, 967.
(14) Kikuchi, H.; Fujii, Y.; Chiba, M.; Mitsudo, S.; Idehara, T.; Tonegawa, T.; Okamoto, K.; Sakai, T.; Kuwai, T.; Ohta, H. *Phys. Rev. Lett.* **2005**, *94*, 227201.
(15) Kang, J.; Lee, C.; Kremer, R. K.; Whangbo, M.-H. *J. Phys.: Condens. Matter* **2009**, *21*, 392201.
(16) Bo, G.; Su, G. *Phys. Rev. Lett.* **2006**, *97*, 089701.
(17) Kikuchi, H.; Fujii, Y.; Chiba, M.; Mitsudo, S.; Idehara, T.; Tonegawa, T.; Okamoto, K.; Sakai, T.; Kuwai, T.; Ohta, H. *Phys. Rev. Lett.* **2006**, *97*, 089702.
(18) Koo, H.-J.; Whangbo, M.-H. *Inorg. Chem.* **2010**, *49*, 9253.
(19) Alexander, A.; Battle, P. D.; Burley, J. C.; Gallon, D. J.; Grey, C. P.; Kim., S. H. *J. Mater. Chem.* **2003**, *13*, 2612.
(20) Soma, M.; Sato, H. *J. Phys. Soc. Jpn.* **2006**, *75*, 124802.
(21) Greedan, J. E. *J. Mater. Chem.* **2001**, *11*, 37 and references cited therein.
(22) Dai, D.; Whangbo, M.-H. *J. Chem. Phys.* **2004**, *121*, 672.
(23) Wu, F.; Kan, E. J.; Tian, C.; Whangbo, M.-H. *Inorg. Chem.* **2010**, *49*, 7545.
(24) Manuel, P.; Adroja, D. T.; Lindgard, P.-A.; Battle, P. D.; Hillier, A. D.; Chapon, L. C.; Son, W.-J.; Whangbo, M.-H. *Phys. Rev. B* Submitted for publication.
(25) Kresse, G.; Hafner, J. *Phys. Rev. B* **1993**, *47*, 558.
(26) Kresse, G.; Furthmüller, J. *Comput. Mater. Sci.* **1996**, *6*, 15.
(27) Kresse, G.; Furthmüller, J. *Phys. Rev. B* **1996**, *54*, 11169.
(28) Perdew, J. P.; Burke, K.; Ernzerhof, M. *Phys. Rev. Lett.* **1996**, *77*, 3865.
(29) Tian, C.; Wibowo, A. C.; zur Loye, H.-C.; Whangbo, M.-H. *Inorg. Chem.* **2011**, *50*, 4142.
(30) Kan, E. J.; Wu, F.; Lee, C.; Kang, J.; Whangbo, M.-H. *Inorg. Chem.* **2011**, *50*, 4182.
(31) Dudarev, S. L.; Botton, G. A.; Savrasov, S. Y.; Humphreys, C. J.; Sutton, A. P. *Phys. Rev. B* **1998**, *57*, 1505.

(32) Dai, D.; Whangbo, M.-H. *J. Chem. Phys.* **2001**, *114*, 2887.
(33) Dai, D.; Whangbo, M.-H. *J. Chem. Phys.* **2003**, *118*, 29.
(34) Xiang, H. J.; Lee, C.; Whangbo, M.-H. *Phys. Rev. B: Rapid Commun.* **2007**, *76*, 220411(R).
(35) Smart, J. S. *Effective Field Theory of Magnetism*; Saunders: Philadelphia, 1966.